

# Estimating Interpretable Heterogeneous Treatment Effect with Causal Subgroup Discovery in Survival Outcomes

Na Bo and Ying Ding

Department of Biostatistics and Health Data Science, University of Pittsburgh

\*Ying Ding: yingding@pitt.edu

## Abstract

Estimating heterogeneous treatment effect (HTE) for survival outcomes has gained increasing attention, as it captures the variation in treatment efficacy across patients or subgroups in delaying disease progression. However, most existing methods focus on post-hoc subgroup identification rather than simultaneously estimating HTE and selecting relevant subgroups. In this paper, we propose an interpretable HTE estimation framework that integrates three meta-learners that simultaneously estimate CATE for survival outcomes and identify predictive subgroups. We evaluated the performance of our method through comprehensive simulation studies across various randomized clinical trial (RCT) settings. Additionally, we demonstrated its application in a large RCT for age-related macular degeneration (AMD), a polygenic progressive eye disease, to estimate the HTE of an antioxidant and mineral supplement on time-to-AMD progression and to identify genetics-based subgroups with enhanced treatment effects. Our method offers a direct interpretation of the estimated HTE and provides evidence to support precision healthcare.

**Keywords:** age-related macular degeneration, interpretable heterogeneous treatment effect, precision medicine, randomized clinical trials, subgroup identification, survival outcomes

## 1 Introduction

Estimating heterogeneous treatment effects (HTE) has gained significant attention in healthcare research, as it captures variations in treatment efficacy across individuals or subgroups exposed to the same treatment. In particular, there is increasing interest in estimating HTE for survival outcomes, which provides a deeper understanding of treatment heterogeneity in disease progression and aids in developing targeted therapeutic strategies tailored to patient-specific characteristics.

HTE is assessed by estimating the conditional average treatment effect (CATE), defined as the expected difference between potential outcomes in treatment and control arms, given patient characteristics. Existing methods for CATE estimation in survival outcomes primarily focus on accurate estimation of CATE and post-hoc subgroup identification. For instance, Bo et al. [2024b,a] employed meta-learners with machine learning to estimate CATE for survival data, identifying beneficial subgroups by selecting thresholds on predicted CATEs and applying variable importance techniques post-hoc. Hu et al. [2021, 2022a] used Bayesian methods to estimate CATE on the median survival time scale, identifying subgroups by examining posterior average survival effects against covariates. Cui et al. [2023] introduced causal survival forests (CSF) to improve the interpretability of CATE estimates through tree structures, although subgroup identification remained challenging due to the complexity of the ensemble trees.

These methods utilizing machine learning techniques often lack interpretability due to their "black box" nature, limiting their interpretations in clinical practice. To address this challenge, there is a growing need for interpretable approaches to CATE estimation. For example, Bargagli-Stoffi et al. [2024] proposed a causal rule ensemble method to estimate CATE for continuous outcomes. Their two-step approach begins by generating potential subgroups using tree-based methods, where predicted CATEs using existing causal inference methods (e.g., causal forests) are used as outcomes and regressed on covariates. In the second step, a penalized regression is applied, where the predicted CATEs are regressed on the generated subgroups. Wu et al. [2023] proposed a similar two-step approach, generating potential subgroups from causal forests and then estimating CATE through D-learner using the generated subgroups as new covariates. Wan et al. [2023a] proposed an interpretable CATE estimation method for continuous outcomes, focusing on the main effects of treatment. They first generated subgroups by regressing inverse probability weighted outcomes on covariates using gradient-boosting trees. Then, they employed an adaptive group lasso to fit observed outcomes to these subgroups. Hiraishi et al. [2024] extended it to incorporate prognostic effects.

Interpretable CATE estimation in survival outcomes remains under-explored. Only recently, Wan et al. [2023b] extended their previous work [Wan et al., 2023a] by using a similar approach based on Cox proportional hazards (Cox PH) model. In this paper, we propose an interpretable HTE estimation framework to estimate CATE in survival outcomes, which not only predicts CATE but also selects important subgroups. Our study is motivated by age-related macular degeneration (AMD), a polygenic and progressive neurodegenerative eye disease that can cause blindness in older individuals. Randomized clinical trials (RCT), known as Age-related Eye Diseases Study (AREDS and AREDS2), evaluated the efficacy of the AREDS formula (an antioxidant and mineral supplement) in delaying AMD progression but showed minimal overall effects. Our previous work [Bo et al., 2024b] estimated CATE of the AREDS formula on time-to-AMD progression and identified key Single Nucleotide Polymorphisms (SNP) using the post-hoc algorithm based on predicted

CATEs. However, this approach only considered individual SNPs, ignoring potential combined effects. In this study, we leverage the interpretability of tree nodes from tree-based algorithms to develop an interpretable framework for estimating CATE in survival outcomes. Instead of using the Cox PH model, which relies on the PH assumption as Wan et al. [2023b] did, we employ inverse probability censoring weighting (IPCW) to handle censored subjects. Our proposed framework utilizes the idea of “pseudo individualized treatment effect” (pseudo-ITE) to address the fundamental causal inference problem, where only one potential outcome is observable. This framework integrates three meta-learners with different statistical properties to construct pseudo-ITE. We evaluated their performance in terms of prediction accuracy and subgroup identification accuracy in various RCT settings through comprehensive simulation studies, providing practical recommendations for implementation. Finally, we applied our proposed method to the AREDS trial to estimate CATE and identify SNP-based subgroups.

The paper is organized as follows. In Section 2, we introduce the notation, assumptions, and target estimand. In Section 3, we describe the proposed method. In Section 4, we examine the proposed method through comprehensive simulations. A real data application is shown to illustrate our proposed method in Section 5. Finally, we make conclusions and discussions in Section 6.

## 2 Notation, assumptions and causal estimand

HTE is defined through CATE. We follow the Neyman–Rubin counterfactual framework [Rubin, 1974, Splawa-Neyman et al., 1990] to define the CATE for survival outcomes. Consider a study of sample size  $n$ , which compares two treatment arms,  $A_i \in \{0, 1\}$  where  $A_i = 1$  denotes taking the treatment and  $A_i = 0$  denotes taking the control for subject  $i$ ,  $i \in \mathcal{I} = \{1, 2, \dots, n\}$ .  $\mathbf{X}_i \in \mathcal{R}^p$  is a  $p$ -dimensional vector of covariates. Let  $T$  denote the survival time and  $C$  denote the censoring time.  $T_i(1)$  and  $T_i(0)$  denote potential survival times;  $C_i(1)$  and  $C_i(0)$  denote potential censoring times;  $\delta_i(1)$  and  $\delta_i(0)$  denote potential event indicators. We define  $U = \min(T, C)$  as the observed time with event indicator  $\delta$  defined as  $\delta = I(T < C)$ . The observed data is denoted as  $D = \{(U_i, \delta_i), A_i, \mathbf{X}_i; i = 1, \dots, n\}$ . In this paper, we define CATE as the expected difference between  $I(T(1) > t^*)$  and  $I(T(0) > t^*)$  given covariates:

$$\tau(\mathbf{x}; t^*) = \mathbb{E}[I(T(1) > t^*) - I(T(0) > t^*) | \mathbf{X} = \mathbf{x}], \quad (1)$$

where  $t^*$  denotes a pre-specified time of interest. CATE can also be defined for other survival quantities. For example, under the restricted mean survival time scale, CATE is defined as  $\tau(\mathbf{x}; t^*) = \mathbb{E}[\min(T(1), t^*) - \min(T(0), t^*) | \mathbf{X} = \mathbf{x}]$ , where  $t^*$  is the restricted time. Similarly, one can define CATE under other transfor-

mation of survival time, e.g.,  $\mathbb{E}[\log(T(1)) - \log(T(0)) | \mathbf{X} = \mathbf{x}]$  (Hu et al. [2022b]).

In this paper, we focus on CATE under the survival probability scale, defined in Equation (1). We assume the following causal analysis assumptions:

- **Assumption 1** (Consistency)  $T_i = A_i T_i(1) + (1 - A_i) T_i(0)$ ,  $C_i = A_i C_i(1) + (1 - A_i) C_i(0)$ ,  $\delta_i = A_i \delta_i(1) + (1 - A_i) \delta_i(0)$
- **Assumption 2** (Unconfoundedness)  $A_i \perp\!\!\!\perp (T_i(0), T_i(1)) | \mathbf{X}_i$ ,  $A_i \perp\!\!\!\perp (C_i(0), C_i(1)) | \mathbf{X}_i$
- **Assumption 3** (Population Overlap):  $e(\mathbf{x}) = P(A_i = 1 | \mathbf{X}_i = \mathbf{x}) \in (0, 1)$

where  $e(\mathbf{x})$  is a propensity score. Given Assumptions 1 to 3, the causal estimand in Equation (1) can be identified as

$$\tau(\mathbf{x}; t^*) = \mathbb{E}[I(T > t^*) | \mathbf{X} = \mathbf{x}, A = 1] - \mathbb{E}[I(T > t^*) | \mathbf{X} = \mathbf{x}, A = 0] = S_1(t^* | \mathbf{x}) - S_0(t^* | \mathbf{x}), \quad (2)$$

where  $S_0(t^* | \mathbf{x})$  and  $S_1(t^* | \mathbf{x})$  are conditional survival probabilities under the control and treatment respectively, given covariates. We also assume the noninformative censoring assumption given covariates and treatment:  $T_i(a) \perp\!\!\!\perp C_i(a) | \mathbf{X}_i, A_i$ .

### 3 Methods

In this section, we introduce the proposed method for estimating interpretable HTE in survival outcomes.

#### 3.1 Problem set-up

Our method is inspired by ‘‘RuleFit’’, proposed by Friedman and Popescu [2008], which constructs an interpretable prediction model through  $y = \beta_0 + \sum_{k=1}^K \beta_k r_k(\mathbf{x}) + \sum_{j=1}^p \alpha_j l_j(\mathbf{x}_j)$ , where  $y$  is any continuous observed outcome collected in a dataset,  $r_k(\mathbf{x}) \in \{0, 1\}$  is the ‘‘rule’’ term for  $k = 1, 2, \dots, K$ ,  $l_j(\mathbf{x}_j)$  is the covariate  $\mathbf{x}_j$  after truncating the possible outliers (e.g., truncate the covariate value of  $\mathbf{X}_j$  at 5% and 95% percentiles of  $\mathbf{X}_j$ ), and  $\beta_k$  and  $\alpha_j$  are the corresponding coefficients. The ‘‘rule’’ terms can be generated from trees. Figure 1A gives an example of the ‘‘rule’’ terms generated from a classification and regression tree by regressing the outcome  $y$  on covariates. By extracting internal and terminal nodes of the tree, rule1 is generated as  $r_1(\mathbf{x}) = I(\text{bmi} = \text{high})$ ; rule2 is generated as  $r_2(\mathbf{x}) = I(\text{bmi} = \text{high})I(\text{age} > 45)$ , etc. Each internal or terminal node can be a candidate rule. One may consider removing complementary rules from this tree (e.g.,  $I(\text{bmi} = \text{high})$  and  $I(\text{bmi} = \text{low})$  are complementary rules.). These rules can be interpreted as subgroups through which each subject can be evaluated whether they satisfy each rule (e.g., fall into this

subgroup). Thus, the covariate space is partitioned into binary indicators (e.g.,  $r_1(\mathbf{x}), r_2(\mathbf{x}), \dots, r_K(\mathbf{x})$ ) using these rules as new covariates. In this paper, we refer to the term "rule" as "candidate subgroup."

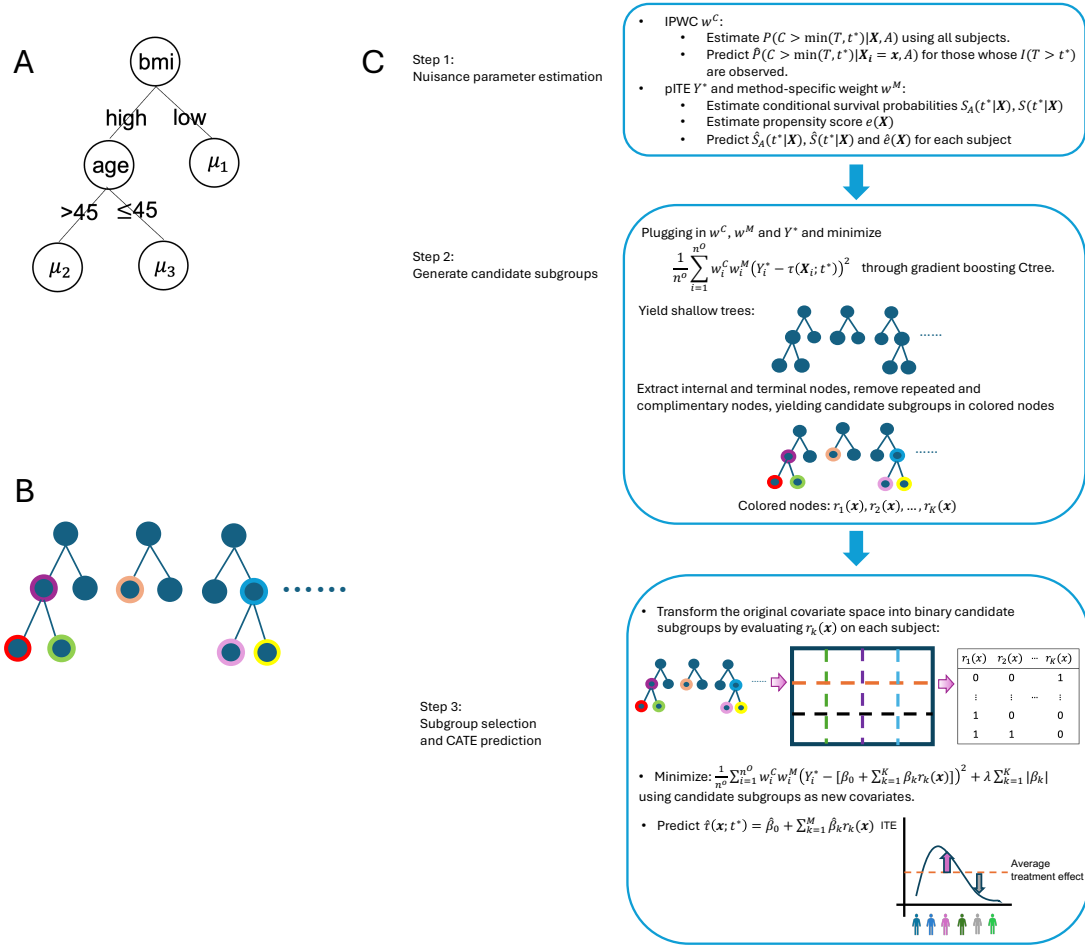


Figure 1: Figure A shows an example of candidate subgroups generated from a single tree. Figure B shows an example of rule extraction from ensembled trees. Figure 3 shows the flow chart of the proposed interpretable meta-learner framework for estimating CATE in survival outcomes.

As seen from the CATE definition in Equation (1), if we can observe individualized treatment effect (ITE)  $I(T_i(1) > t^*) - I(T_i(0) > t^*)$  for each subject  $i$ , interpretable CATE can be estimated through a model similar to "RuleFit", using ITE to regress on candidate subgroups. However, the "outcome" here is ITE, which is unobservable due to two reasons. Firstly, only one of the potential outcomes in  $I(T(1) > t^*) - I(T(0) > t^*)$  can be observed even without censoring as patients cannot take treatment and control simultaneously. Secondly, when censoring occurs,  $I(T > t^*)$  cannot be observed for those who are censored before the time of interest  $t^*$ . In this paper, we utilize an idea of pseudo-ITE, proposed in our previous work [Bo et al., 2024a], to solve this problem, which replaces unobservable ITE with pseudo-ITE that can be constructed using observed data. In the next section, we introduce our proposed method. In Section 3.3,

we explain how pseudo-ITE is constructed.

### 3.2 An interpretable HTE estimation framework to estimate CATE in survival outcomes

In our previous work [Bo et al., 2024a], we proposed a pseudo-ITE-based framework to estimate CATE for survival outcomes by minimizing a weighted squared error loss:

$$\frac{1}{n} \sum_{i=1}^n w_i^M (Y_i^* - \tau(\mathbf{X}_i; t^*))^2,$$

where  $Y^*$  is a constructed pseudo-ITE (pITE) which replaces the unobservable ITE.  $w^M$  is a method-specific weight corresponding to the method for constructing  $Y^*$ . There are multiple ways to construct  $Y^*$ . For example, by using the inverse probability weighting (IPW) method, we can construct  $Y^* = \frac{A-e(\mathbf{X})}{e(\mathbf{X})(1-e(\mathbf{X}))} I(T > t^*)$  with  $w^M = 1$ , which satisfies  $\tau(\mathbf{x}; t^*) = E[Y^* | \mathbf{X} = \mathbf{x}, t^*]$ . Note that  $Y^*$  utilizes observed outcome  $I(T > t^*)$ , but  $I(T > t^*)$  cannot be observed (e.g., cannot be constructed) for those who are censored before the time  $t^*$ . To accommodate, we use IPCW by predicting  $w^C = \frac{1}{P(C > \min(T, t^*) | \mathbf{X}, A)}$  for those whose  $I(T > t^*)$  can be observed. Thus, the objective function becomes

$$\frac{1}{n^o} \sum_{i=1}^{n^o} w_i^C w_i^M (Y_i^* - \tau(\mathbf{X}_i; t^*))^2, \quad (3)$$

where  $n^o$  denotes the sample size of complete data  $D^o = \{(U_i, \delta_i), A_i, \mathbf{X}_i; i \in \mathcal{I}^o\}$  whose  $I(T > t^*)$  is known (for individuals who are censored before  $t^*$ , their  $I(T > t^*)$  are unknown and thus not in  $D^o$ ), denoted as  $\mathcal{I}^o = \{i \in \mathcal{I} : U_i > t^* \text{ or } (U_i \leq t^* \text{ and } \delta_i = 0)\}$ .

Suppose we have  $K$  candidate subgroups,  $r_1(\mathbf{x}), r_2(\mathbf{x}), \dots, r_K(\mathbf{x})$ , that may potentially contribute to CATE prediction. We can re-parameterize  $\tau(\mathbf{X}_i; t^*)$  in the objective function (3) as  $\tau(\mathbf{x}; t^*) = \beta_0 + \sum_{k=1}^K \beta_k r_k(\mathbf{x})$  for  $k = 1, 2, \dots, K$ . Thus, our proposed interpretable framework solves CATE in survival outcomes by minimizing the following objective function:

$$\frac{1}{n^o} \sum_{i=1}^{n^o} w_i^C w_i^M \{Y_i^* - [\beta_0 + \sum_{k=1}^K \beta_k r_k(\mathbf{x}_i)]\}^2 + \lambda \sum_{k=1}^K |\beta_k|, \quad (4)$$

where  $r_k(\mathbf{x}_i) \in \{0, 1\}$  denotes whether a subject  $i$  with covariate  $\mathbf{x}_i$  falls into the  $k$ -th candidate subgroup or not;  $\beta_k$  denotes the coefficient of the corresponding candidate subgroup  $r_k(\mathbf{x}_i)$ . Lasso penalty is applied to select important subgroups contributing to CATE with a tuning parameter  $\lambda$ . In the following, we describe the specific steps in solving the objective function (4) with a flowchart in Figure 1C for illustration.

**Step 1: Nuisance parameter estimation.** The objective function (4) involves nuisance parameters from three sources –  $P(C > \min(T, t^*)|\mathbf{X}, A)$  in  $w^C$ , nuisance parameters in the construction of  $Y^*$  (e.g., propensity score  $e(\mathbf{x})$  in the IPW method) and nuisance parameters in the method-specific weight  $w^M$ . Censoring probability can be estimated using KM if censoring is completely independent of survival time (i.e.,  $T \perp C$ ) or using random survival forests (RSF) if censoring is covariate-dependent (i.e.,  $T \not\perp C$  but  $T \perp C|\mathbf{X}, A$ ). Method-specific weight  $w^M$  and pITE  $Y^*$  involve estimating propensity score  $e(\mathbf{X})$  and some other survival quantities (e.g., conditional survival probabilities in each treatment arm  $S_A(t^*|\mathbf{X})$ ). Parametric or semi-parametric methods can be applied (e.g., RF for estimating propensity score  $e(\mathbf{X})$ , RSF for estimating conditional survival probabilities  $S_a(t^*|\mathbf{X})$  or  $S(t^*|\mathbf{X})$ ). If the sample size is large, sample splitting can be used in which we split data into two folds, as implemented in Kennedy [2020]. The first fold is used to estimate nuisance parameters; the second fold is used to construct  $Y^*$  and  $w^M$  with estimated nuisance parameters from the first fold and proceed with Step 2. If the sample size is moderate or scarce, cross-fitting is recommended to estimate nuisance parameters [Chernozhukov et al., 2018].

**Step 2: Generate candidate subgroups.** After plugging in nuisance parameters, we minimize the objective function (3) (with respect to  $\tau(\mathbf{X}_i; t^*)$ ) using a tree-based method. This will transform the original covariate space  $\mathbf{X} \in \mathcal{R}^p$  into candidate subgroups  $\mathbf{r}(\mathbf{x})$ . In the generated trees, each internal and terminal node is a candidate subgroup. Complementary subgroups (i.e.,  $r_j(\mathbf{x}) + r_l(\mathbf{x}) = 1$  for  $i \neq l$ ) and repeated subgroups are removed. Ensembled trees can be used to extract tree nodes to cover as much of the covariate space as possible. Figure 1B shows an example of candidate subgroups generated from trees, denoted as the colored nodes.

In this work, we propose to generate candidate subgroups by minimizing the objective function (3) through the conditional inference tree (CTree)[Hothorn et al., 2006]. CTree employs the unbiased splitting criteria in which it decides whether any information of the outcome is carried by each covariate when splitting at each internal node. Specifically, at each splitting node, it tests the hypothesis  $H_0^j : P(Y^*|\mathbf{X}_j) = P(Y^*)$  with the global null hypothesis  $H_0 : \bigcap_{j=1}^p H_0^j$ . The partial hypothesis is tested through permutation tests. Multiple testing adjustments can be applied (e.g., Bonferroni corrections). The tree stops splitting if the global null hypothesis is not rejected at pre-specified level  $\alpha$ . Note that CTree is already unbiased splitting without multiple testing adjustments. This unbiased splitting criterion enhances the ability of trees to split on covariates that truly contribute to CATE. More details can be found in their original paper [Hothorn et al., 2006]. In this paper, gradient boosting is used to build ensembled CTrees, which not only partitions the covariate space as much as possible but also makes the candidate subgroups more interpretable by building shallow trees. After building gradient boosting CTrees, all terminal and internal nodes are extracted with complementary and repeated nodes removed. We use  $r_1(\mathbf{x}), r_2(\mathbf{x}), \dots, r_K(\mathbf{x})$  to denote the candidate

subgroups.

**Step 3: Subgroup selection and CATE prediction.** We evaluate whether each subject satisfies each candidate subgroup generated in Step 2, yielding 0 or 1 for each  $r_k(\mathbf{x})$ . We then input  $r_1(\mathbf{x}), r_2(\mathbf{x}), \dots, r_K(\mathbf{x})$  as new covariates into the objective function (4) and solve for  $\beta$ 's by applying Lasso penalty with cross-validation (CV) for selecting the tuning parameter  $\lambda$ . The subgroups are decided based on the selected  $\lambda$ , which makes the best predictions in terms of the smallest mean squared errors through the CV. The predicted CATE is  $\hat{\tau}(\mathbf{x}; t^*) = \hat{\beta}_0 + \sum_{k=1}^M \hat{\beta}_k r_k(\mathbf{x})$ , where  $r_k(\mathbf{x})$  are selected subgroups. Let  $R_k$  ( $k = 1, 2, \dots, M$ ) and  $V_j$  ( $j = 1, 2, \dots, p$ ) denote the subgroup importance and variable importance, calculated as:

$$R_k = |\hat{\beta}_k| \cdot \sqrt{s_k(1 - s_k)}, \quad V_j = \sum_{X_j \in r_k} \frac{R_k}{c_k}, \quad (5)$$

where  $s_k = \frac{1}{n^o} \sum_{i=1}^{n^o} r_k(\mathbf{x}_i)$  denotes the support of subgroup  $r_k$  and  $c_k$  denotes the number of subgroups that contain  $X_j$ .

### 3.3 Construction of pITE

In this section, we describe how pITE  $Y^*$  and its method-specific weight  $w^M$  can be constructed. In our previous paper [Bo et al., 2024a], we introduced six methods in Table 2, referred to as "meta-learners", that construct pITE with different statistical properties. In this paper, we include only three meta-learners that have the double robustness feature.

**DR-learner.** Kennedy [2020] proposed a doubly-robust learner (DR-learner) derived from the efficient influence curve to estimate the average treatment effect, in which:

$$Y_{DR}^* = \frac{A - \hat{e}(\mathbf{X})}{\hat{e}(\mathbf{X})(1 - \hat{e}(\mathbf{X}))} \left( I(T > t^*) - \hat{S}_A(t^*|\mathbf{X}) \right) + \hat{S}_1(t^*|\mathbf{X}) - \hat{S}_0(t^*|\mathbf{X}).$$

It satisfies  $\tau(\mathbf{x}; t^*) = E[Y^*|\mathbf{X} = \mathbf{x}, t^*]$  and does not require method-specific weight  $w^M$  (e.g.,  $w^M = 1$  for each subject). The subscript of  $Y^*$  denotes the abbreviation of each meta-learner.

**DEA-learner.** Chen et al. [2017] proposed DEA-learner by extending D-learner [Tian et al., 2014], also called a modified covariate approach. The original objective function of D-learner solves CATE in a parametric form through minimizing the objective function:

$$\min_{\tau} \left[ \frac{1}{n^o} \sum_{i=1}^{n^o} \frac{(2A_i - 1)(A_i - e(\mathbf{X}_i))}{e(\mathbf{X}_i)(1 - e(\mathbf{X}_i))} \left( I(T_i > t^*) - \frac{2A_i - 1}{2} \mathbf{X}_i \gamma \right)^2 \right],$$



where  $\tau(\mathbf{X}_i; t^*) = \mathbf{X}_i \gamma$  and the modified covariates becomes  $\frac{2A_i-1}{2} \mathbf{X}_i$ . Chen et al. [2017] modified D-learner by replacing the observed outcome ( $I(T > t^*)$ ) with its residual ( $I(T > t^*) - S(t^*|\mathbf{X})$ ). Here we assume a non-parametric form of  $\tau(\mathbf{x}; t^*)$  and rearrange its objective function to get  $Y_{DEA}^* = 2(2A - 1) \left( I(T > t^*) - \hat{S}(t^*|\mathbf{X}) \right)$  and  $w^M = (2A - 1) \frac{A - e(\mathbf{X})}{4e(\mathbf{X})(1 - e(\mathbf{X}))}$ .

**R-learner.** Nie and Wager [2020] proposed R-learner using Robinson’s decomposition:  $I(T_i > t^*) - E[I(T_i > t^*)|\mathbf{X}_i = \mathbf{x}, t^*] = (A_i - e(\mathbf{X}_i)) \tau(\mathbf{X}_i; t^*) + \varepsilon_i$ , where  $E[\varepsilon_i|\mathbf{X}_i, A_i] = 0$ . Then, CATE is solved by minimizing the objective function:

$$\min_{\tau} \left\{ \frac{1}{n^o} \sum_{i=1}^{n^o} [(I(T_i > t^*) - S(t^*|\mathbf{X}_i)) - (A_i - e(\mathbf{X}_i)) \tau(\mathbf{X}_i; t^*)]^2 \right\},$$

where  $S(t^*|\mathbf{X})$  is the survival function ignoring the treatment groups. We can rewrite the objective function to get  $Y_{RL}^* = \frac{I(T > t^*) - \hat{S}(t^*|\mathbf{X})}{A - \hat{e}(\mathbf{X})}$  and  $w^M = (A - \hat{e}(\mathbf{X}))^2$ .

DR, DEA, and R- learners have the double robustness property in which  $\tau(\mathbf{x}; t^*)$  can be consistently estimated if the propensity score ( $e(\mathbf{x})$ ) or mean outcome regression models ( $S_A(t^*|\mathbf{X})$ ,  $S(t^*|\mathbf{X})$ ) are consistently estimated. More details on the derivation and properties of  $Y^*$  and  $w^M$  can be found in our previous paper [Bo et al., 2024a].

## 4 Simulations

In this section, we performed comprehensive simulations under multiple study designs, considering low-dimensional independent and high-dimensional correlated signals.

### 4.1 Simulation designs

We first considered an independent signal setting with ten independent covariates.  $X_1, X_2, \dots, X_5$  were binary covariates created by  $X_j = I(\tilde{X}_j > 0)$ , where  $\tilde{X}_j$  was independently generated from a Normal distribution  $N(0, 1)$  for  $j = 1, 2, \dots, 5$ , and  $X_6, X_7, \dots, X_{10}$  were continuous covariates independently generated from  $N(0, 1)$  for  $j = 6, 7, \dots, 10$ . Treatment assignment was determined by the propensity score:  $\text{logit}(e(\mathbf{X})) = 0.4 - 0.3X_1 - 0.2X_6 - 0.3X_2 - 0.35X_7 - 0.2X_3 - 0.25X_8$ . The sample sizes of the two treatment arms are roughly equal.

Potential survival times were simulated from a Weibull regression model:  $T(a|\mathbf{X}) = \lambda_a \left\{ \frac{-\log(U)}{\exp\{f_a(\mathbf{X})\}} \right\}^{\frac{1}{\eta}}$ , where  $U \sim \text{Unif}[0, 1]$ .  $f_a(\mathbf{X}) = b(\mathbf{X}) + a * h(\mathbf{X})$  introduced the source of HTE.  $b(\mathbf{X})$  was a baseline function shared between two treatment arms;  $h(\mathbf{X})$  introduced arm-specific treatment effect. We considered simple

to complex scenarios of  $b(\mathbf{X})$  and  $h(\mathbf{X})$  listed below:

$$\begin{aligned}
\text{S1: } b(\mathbf{X}) &= 2X_6 - 1.2X_7, \\
h(\mathbf{X}) &= 2.8X_1 + 1.4X_2. \\
\text{S2: } b(\mathbf{X}) &= 1.6X_1 - 1.4X_6 - 1.2X_7, \\
h(\mathbf{X}) &= 2.5X_1 - 1.8X_2 - 2X_3. \\
\text{S3: } b(\mathbf{X}) &= 1.6X_1 - 1.4X_6 - 1.2X_7 - X_1X_7 - 0.8X_8^2, \\
h(\mathbf{X}) &= 2.5X_1 - 1.8X_2 - 2X_3 - 1.4X_1X_3.
\end{aligned}$$

In scenario 1, the covariates are in the linear form and do not share between  $b(\mathbf{X})$  and  $h(\mathbf{X})$ . In scenario 2, we added one shared covariate in both  $b(\mathbf{X})$  and  $h(\mathbf{X})$ . In scenario 3, we considered the nonlinear form and interaction of the covariates in both  $b(\mathbf{X})$  and  $h(\mathbf{X})$ . Under this setting, around half of the covariates are independent noise variables that do not contribute to either  $b(\mathbf{X})$  or  $h(\mathbf{X})$ . The shape parameter was set as  $\eta = 2$ ; scale parameter was set as  $\lambda_0 = 16, 20, 20$  and  $\lambda_1 = 26, 22, 22$  for scenario 1 to 3 respectively. Censoring time was simulated independently from exponential distribution to guarantee a 30% censoring rate with the rate parameter as  $r = 0.018, 0.019, 0.01$  for scenario 1 to 3.

Additionally, we considered high-dimensional correlated signal settings. We generated covariates from a multivariate normal distribution  $\tilde{\mathbf{X}} \sim MVN(\mathbf{0}, 0.5\Sigma)$ , where  $\Sigma = \{\sigma_{jj'} = e^{-|j-j'|}, 1 \leq j, j' \leq p\}$  for  $p = 100$ .  $X_1, X_2, X_3, X_4, X_5, X_{11}, X_{12}, \dots, X_{55}$  are binary covariates created by  $X_j = I(\tilde{X}_j > 0)$  for  $j = 1, 2, 3, 4, 5, 11, 12, \dots, 55$  and the rest of are continuous with  $X_j = \tilde{X}_j$ .

We generated 100 training datasets of sample size  $n = 1,000$  and one test data of sample size  $N = 10,000$ . Our earlier work studied the performance of different machine learning methods to estimate nuisance parameters in meta-learners [Bo et al., 2024b]. We chose to use RSF to estimate  $S_a(t^*|\mathbf{X})$  and  $S(t^*|\mathbf{X})$  and RF to estimate  $e(X)$ , which demonstrated satisfactory performance. KM was used to estimate  $P(C > \min(T, t^*))$  as censoring is completely independent of survival time in the simulations. If censoring may depend on covariates, we suggest using model-based or machine learning methods (e.g., RSF) to estimate the censoring probability. We also examined the performance under the high censoring rate (e. g., 50% to 70%) and covariate-dependent censoring settings in the Supplemental Materials. A gradient boosting algorithm coupled with CTree was performed to generate ensembled shallow trees. The tree depth was set as 5. Bonferroni correction in CTree was implemented with  $\alpha = 0.1$ . No multiple testing adjustment was also conducted for the high-dimensional correlated signal setting. We compared the performance of three meta-learners to the case when pITE  $Y^*$  was generated directly using the predicted  $\hat{\tau}(\mathbf{x}; t^*)$  from CSF and

Bayesian accelerated failure time model (BAFT).

## 4.2 Evaluation metrics

**Prediction performance.** Let  $\mathcal{G} = \{G_1, G_2, \dots, G_Q\}$  denote  $Q$  numbers of groups. We evaluated CATE predictions in a subgroup by dividing the predictions into  $Q$  bins based on the ordering of true CATEs. We set  $Q = 50$  here. We evaluated the performance of meta-learners using Bias, binned-RMSE, and Spearman rank correlation, defined as:

$$\begin{aligned} \text{Bias} &= \frac{1}{N} \sum_{i=1}^N (\hat{\tau}_i(\mathbf{x}; t^*) - \tau_i(\mathbf{x}; t^*)), \\ \text{binned-RMSE} &= \frac{1}{Q} \sum_{q=1}^Q \sqrt{\frac{1}{N_q} \sum_{i=1}^{N_q} (\hat{\tau}_i(\mathbf{x}; t^*) - \tau_i(\mathbf{x}; t^*))^2}, \\ \text{Spearman Corr} &= 1 - \frac{6 \sum d_i^2}{N(N^2 - 1)}, \end{aligned}$$

where  $\tau_i(\mathbf{x}; t^*)$  and  $\hat{\tau}_i(\mathbf{x}; t^*)$  denote the true CATE and predicted CATE for subject  $i$ , and  $d_i$  denotes the difference between the ranks of  $\tau_i(\mathbf{x}; t^*)$  and  $\hat{\tau}_i(\mathbf{x}; t^*)$  in testing data.

**Subgroup identification accuracy.** We evaluated each method’s ability to select the correct covariates that contribute to CATE prediction (e.g.,  $X_j$ ’s in  $b(\mathbf{X})$  and  $h(\mathbf{X})$ ). We calculated the number of times among 100 simulations that each covariate was ever used to formulate any selected subgroups. We colored the signal covariates in  $b(x)$  and  $h(x)$ , respectively. In addition, we also examined the sparseness of the selected subgroups by summarizing the number of finally selected subgroups among 100 simulations.

## 4.3 Simulation results

### 4.3.1 Independent signal setting

Figure 2 shows prediction performance under the independent signal setting with Bonferroni corrections ( $\alpha = 0.1$ ) in CTree for generating candidate subgroups. In scenario 1, DEA-learner and BAFT produce minimal biases compared to other methods. In scenario 2 and 3, biases increase slightly for all methods except BAFT, which maintains the smallest bias. Using predicted CATEs from CSF shows the largest bias, particularly in complex scenarios (scenarios 2 and 3). All methods show comparable RMSEs and high correlations with true CATEs, where BAFT slightly outperforms the others. Overall, when using three meta-learners to construct  $Y^*$  under our framework, they show similar prediction accuracy to the case when  $Y^*$  is generated as predicted CATE from BAFT.

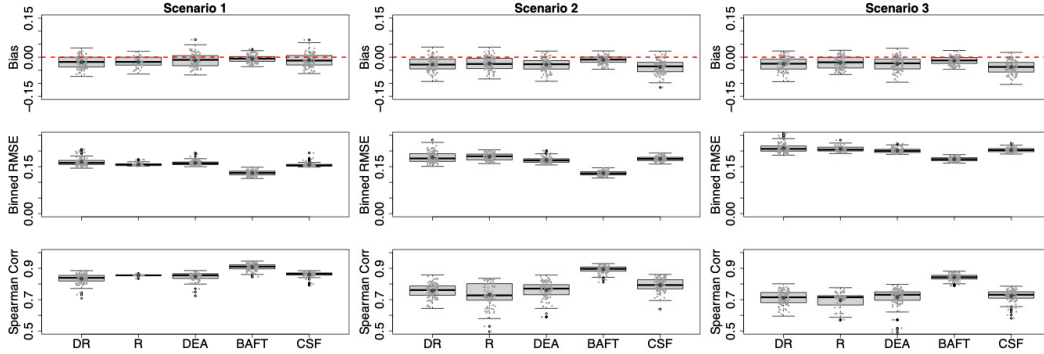


Figure 2: Prediction accuracy under the independent signal setting. The predictions performance under the following meta-learners were examined: DR-learner (DR), R-learner(R) and DEA-learner (DEA). ‘CSF’ represents causal survival forests. ‘BAFT’ represents Bayesian accelerated failure time model. Bonferroni correction with  $\alpha = 0.1$  was performed in generating candidate subgroups using gradient boosting CTree. The upper panel shows biases; the middle panel shows binned-RMSEs; the lower panel shows Spearman rank correlations.

Figure 3 shows the number of times that each covariate is ever used in any selected subgroup among 100 simulations. With DEA-learner, the covariates in  $h(\mathbf{X})$  (those directly contributing to CATE) are frequently used to form selected subgroups (100% for  $X_1$ ,  $> 60\%$  for  $X_2$ ), while the covariates in  $b(\mathbf{X})$  appear in about 40% of simulations. Noise covariates are less picked to form subgroups ( $< 10\%$ ) in all three scenarios. DR-learner tends to use noise covariates more frequently in all scenarios. BAFT, despite its good prediction accuracy, uses all noise covariates in all simulations. Note that there are no candidate subgroups generated from CTree when  $Y^*$  is constructed by R-learner in around 50%, 5%, and 20% simulations in scenario 1, 2, and 3, respectively. The major reason is that CTree stops splitting as no covariate passes the Bonferroni correction threshold. Under R-learner, there are around 3% simulations in which gradient boosting CTree generates more than one candidate subgroups but yield no subgroups after Lasso penalization. Thus, the frequencies of covariates under R-learner are lower than other methods.

The upper panel of Table 1 summarizes the number of selected subgroups under each method. DEA-learner retains the sparseness, selecting 3 to 10 median number of subgroups among 100 simulations. DR-learner also retains some sparseness but selects more subgroups than the DEA-learner (the median number of selected subgroups is between 9 and 24). BAFT and CSF select more than 100 subgroups that contain a lot of noise covariates. In addition, the effects of these selected subgroups under BAFT and CSF are very small (e.g.,  $\hat{\beta}_k < 0.01$  for most coefficients). We still see similar results with a more strict Bonferroni correction criterion ( $\alpha = 0.05$ ) in solving CTree to generate candidate subgroups (results are not shown).

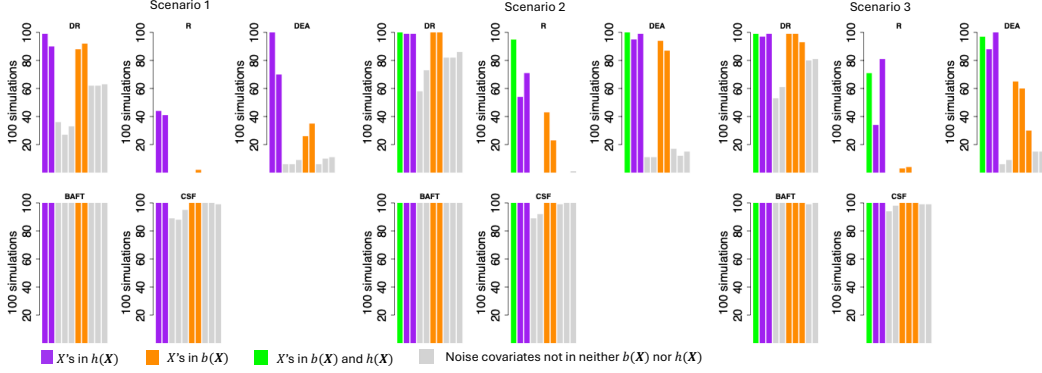


Figure 3: Variable detection under the independent signal setting. The histogram shows the number of times that each covariate is ever used to formulate any selected subgroups among 100 simulations. Purple represents covariates in  $h(\mathbf{X})$ ; orange represents covariates in  $b(\mathbf{X})$ ; green represents covariates shared between  $h(\mathbf{X})$  and  $b(\mathbf{X})$ ; grey represents noise covariates that are not in neither  $b(\mathbf{X})$  nor  $h(\mathbf{X})$ . The predictions performance under the following meta-learners were examined: DR-learner (DR), R-learner (R) and DEA-learner (DEA). ‘CSF’ represents causal survival forests. ‘BAFT’ represents Bayesian accelerated failure time model. Bonferroni correction with  $\alpha = 0.1$  was performed in generating candidate subgroups using gradient boosting CTree.

Table 1: The number of selected subgroups under each method in the independent (Bonferroni correction  $\alpha = 0.1$  in gradient boosting CTree) and the high-dimensional correlated signal setting ( $\alpha = 0.01$  without Bonferroni correction in gradient boosting CTree) in 100 simulations, median (min, max).

	DR	R	DEA	BAFT	CSF
Independent Signals					
Scenario 1	9 (0, 34)	0 (0, 5)	3 (1, 12)	142 (88, 181)	125 (79, 168)
Scenario 2	24 (4, 65)	3 (0, 8)	10 (3, 19)	212 (151, 270)	191 (134, 291)
Scenario 3	21 (0, 63)	2 (0, 6)	7 (1, 14)	168 (123, 209)	152 (102, 254)
Weakly Correlated Signals ( $p=100$ )					
Scenario 1	585 (403, 694)	0 (0, 4)	24 (3, 43)	445 (361, 510)	381 (296, 559)
Scenario 2	623 (40, 169)	2 (0, 7)	26 (5, 53)	511 (435, 622)	499 (363, 631)
Scenario 3	609 (435, 716)	2 (0, 5)	28 (3, 60)	462 (358, 538)	432 (304, 660)

### 4.3.2 High-dimensional correlated signal setting.

Figure 4 shows the prediction accuracy under the correlated signal setting. Unlike the low-dimensional independent signal setting,  $\alpha$  was set as 0.01 without Bonferroni corrections for generating candidate subgroups in CTree. Since the number of covariates is large and correlated, Bonferroni corrections (even with a larger  $\alpha$ ) may result in no candidate subgroups. Similar to the independent signal setting, DR- and DEA-learners show minimal biases in scenario 1 but slightly larger biases in scenarios 2 and 3. BAFT shows the smallest biases compared to other methods in all three scenarios. CSF shows larger biases compared to all the other methods, especially in scenarios 2 and 3. DR-learner yields the largest RMSEs and lowest correlations with true CATEs in all scenarios, while other methods show comparable RMSEs and correlations.

Figure 5 shows the number of times that each covariate is ever used to formulate any selected subgroup

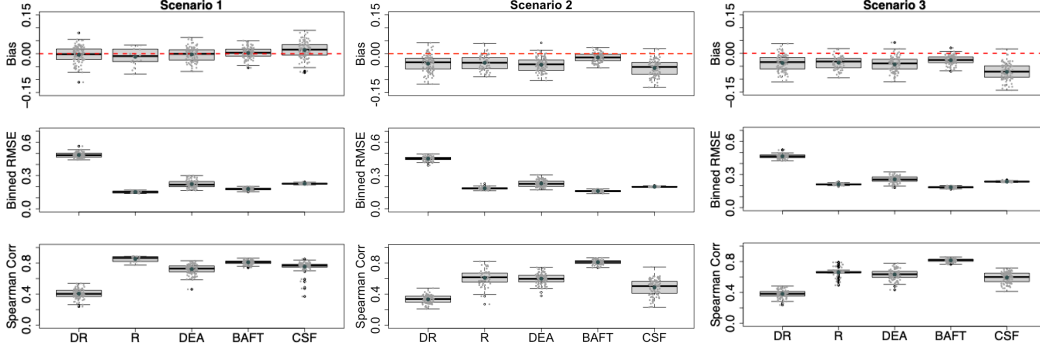


Figure 4: Prediction accuracy under the high-dimensional correlated signal setting. The prediction performance under the following meta-learners were examined: DR-learner (DR), R-learner (R) and DEA-learner (DEA). ‘CSF’ represents causal survival forests. ‘BAFT’ represents Bayesian accelerated failure time model.  $\alpha$  was set as 0.01 without Bonferroni corrections for generating candidate subgroups using gradient boosting CTree. The Upper panel shows biases; the middle panel shows binned-RMSEs; the lower panel shows Spearman rank correlations.

in 100 simulations. Similar to the independent signal setting, for DEA-learner, covariates in  $h(\mathbf{X})$  are chosen to form subgroups in over 80% simulations, while noise covariates are rarely used, evidenced by low detection frequencies, particularly in scenario 2 and 3. It also uses covariates in  $b(\mathbf{X})$  with moderate frequencies. DR-learner, BAFT and CSF use a lot of noise covariates to form subgroups. Note that R-learner only generates one candidate subgroup in 80%, 40%, and 30% simulations from scenario 1 to 3, respectively. Thus, these simulations were not included in the evaluation as the Lasso penalty requires at least two covariates as input. R-learner barely picks any noise variables, but it also does not pick the signal variables frequently. In the lower panel of Table 1, DEA-learner retains the sparseness of selected subgroups, while DR-learner, BAFT, and CSF yields more than 400 subgroups with small effects. R-learner fails to generate subgroups (median number of selected subgroups is 0 to 2). We see similar results when Bonferroni corrections were performed.

In summary, under both low-dimensional independent and high-dimensional correlated signal settings, DEA-learner performs the best in terms of selecting sparse subgroups with correct covariates contributing to CATE while retaining good prediction accuracy. Note that in the high-dimensional correlated signal settings, if Bonferroni corrections are used in CTree, although DEA-learner still shows the best performance, there are around 20% simulations that no candidate subgroups are generated in scenario 1; in scenarios 2 and 3, this issue is largely reduced, but there are around 20% simulations that yield no final selected subgroups after Lasso penalization. Thus, with high-dimensional correlated signals, we recommend using a relaxed Bonferroni correction threshold (e.g.,  $\alpha = 0.2$ ) or not using multiple testing adjustments but choosing a smaller  $\alpha$  (e.g.,  $\alpha = 0.01$ ).

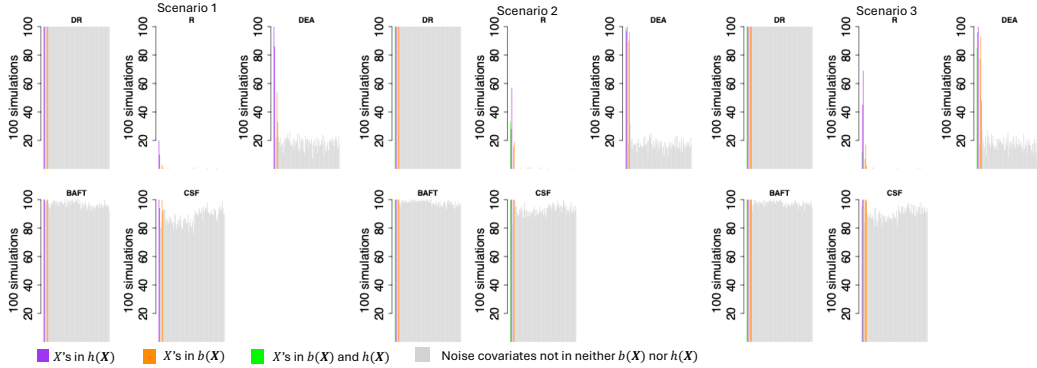


Figure 5: Variable detection under the high-dimensional correlated signal setting. The histogram shows the number of times that each covariate is ever used to formulate any selected subgroups among 100 simulations. Purple represents covariates in  $h(\mathbf{X})$ ; orange represents covariates in  $b(\mathbf{X})$ ; green represents covariates shared between  $h(\mathbf{X})$  and  $b(\mathbf{X})$ ; grey represents noise covariates that are not in neither  $b(\mathbf{X})$  nor  $h(\mathbf{X})$ . The prediction performance under the following meta-learners were examined: DR-learner (DR), R-learner (R) and DEA-learner (DEA). ‘CSF’ represents causal survival forests. ‘BAFT’ represents Bayesian accelerated failure time model.  $\alpha$  was set as 0.01 without Bonferroni corrections for generating candidate subgroups using gradient boosting CTree.

## 5 Real data application

### 5.1 Data description

In this study, we analyzed data from two AREDS clinical trials. The AREDS trial served as our training dataset and the subsequent AREDS2 trial served as test data. We analyzed 806 patients in AREDS data diagnosed with AMD and free of late AMD in at least one eye at the enrollment, categorized as AMD stages 2, 3, or 4. As shown in Table 2, patients were randomized based on their baseline characteristics and followed for 10 years, with 415 (51.49%) randomized to the AREDS formula arm (treatment) and 391 (48.51%) to the placebo arm (control). The study population had a mean age of 68.77 years (SD = 5.05), 466 (57.82%) female and 393 (48.76%) non-smokers. Patients included in AREDS had mild-to-moderate AMD with approximately half (56.70%) of the patients having moderate AMD and a mean baseline AMD severity scale as 4.09 (SD = 2.06). In addition to the baseline characteristics, we included 46 SNPs (denoted as ‘CE4’ SNPs) which were identified to be associated with treatment efficacy [Wei et al., 2021] and 67 prognostic SNPs which were reported to be associated with AMD progression [Yan et al., 2018] (top SNPs with  $p < 10^{-5}$ ).

AREDS2 was a subsequent clinical trial that focused on patients with more severe AMD for a 6-year follow-up. It examined the efficacy of four treatment arms (no placebo arm), including 112 patients randomized to the original AREDS formula. These patients in the AREDS formula arm had a mean baseline

Table 2: Baseline characteristics of the AREDS and AREDS2 data used in the analysis.

Number of subjects	All ( <i>n</i> = 806)	Placebo ( <i>n</i> = 391)	AREDS trial	<i>p</i> -value*	AREDS2 trial
			Antioxidants and Zinc (AREDS formula) ( <i>n</i> = 415)		Antioxidants and Zinc ( <i>n</i> = 112)
Age				0.4905	
Mean (SD)	68.77 (5.05)	68.90 (5.17)	68.66 (4.93)		71.29 (7.25)
Median (Range)	68.60 (55.30-81.00)	68.50 (55.30-81.00)	68.70 (55.50-79.50)		71.00 (53.00, 86.00)
Sex (n, %)				0.8236	
Female	466 (57.82)	224 (57.29)	242 (58.31)		50 (44.64)
Male	340 (42.18)	167 (42.71)	173 (41.69)		62 (55.36)
Smoking (n, %)				0.6877	
Never Smoked	393 (48.76)	194 (49.62)	199 (47.95)		44 (39.29)
Former/Current Smoker	413 (51.24)	197 (50.38)	216 (52.05)		68 (60.71)
Baseline AREDS AMD severity score				0.6303	
Mean (SD)	4.09 (2.06)	4.13 (2.06)	4.06 (2.07)		5.43 (0.96)
Median (Range)	4 (1-8)	4.00 (1-8)	4 (1-8)		6.00 (2.00, 6.00)

\**p*-value is based on two-sample *t*-test or Chi-square test for continuous or categorical variables.

severity scale of 5.43 (SD = 0.96), mean age of 71.29 (SD = 7.25), 50 (44.64%) females and 44 (39.29%) non-smokers, which were similar to the AREDS cohort (right column of Table 2). We analyzed 110 patients after excluding two patients who had missing SNP values.

## 5.2 Interpretable prediction of CATE of AREDS formula on time-to-AMD progression

In this section, we applied the proposed interpretable HTE estimation framework to AREDS clinical trials to estimate CATE on time-to-AMD progression. The time of interest was five years. DEA-learner for constructing pITE was used under our proposed framework, which is the best performer under the weakly-correlated signal setting with a large number of noise variables. AREDS was used to train the model, and AREDS2 was used as the test data. No multiple testing adjustments with  $\alpha = 0.01$  were performed to generate candidate subgroups through gradient boosting CTree as recommended by our simulation studies. The tuning parameters in CTree were set the same as that in simulations.

Figure 6 shows the subgroups identified by training the model on AREDS. Fifteen subgroups were identified to be predictive of CATE in delaying time-to-AMD progression. Twelve SNPs, the baseline AMD severity scale, and education formulate these fifteen subgroups, in which all SNPs are CE4 SNPs, except that *rs59182762* (*EFCAB14, CYP4B1*, CHR 1) is a prognostic SNP. Among the eleven CE4 SNPs, five are from CHR 14 (*rs1056437, rs11626491, rs4903476, rs77000175, rs141472150*), two are from CHR 10 (*rs1618927, rs1871453*), two are from CHR 5 (*rs149309589, rs71594472*), one is from CHR 3 (*rs9815579*), and one is from CHR 19 (*rs141380308*). Among the fifteen subgroups, eleven subgroups are constructed by two or more SNPs and baseline covariates. The subgroups with positive estimated coefficients (colored orange) are beneficial subgroups with enhanced treatment effects, while those with negative estimated coefficients (colored blue) are “adverse” subgroups with worse treatment effects. Thus, the complementary of those “adverse” subgroups are beneficial subgroups. The right column of Figure 6 shows the subgroup size



on AREDS trial.

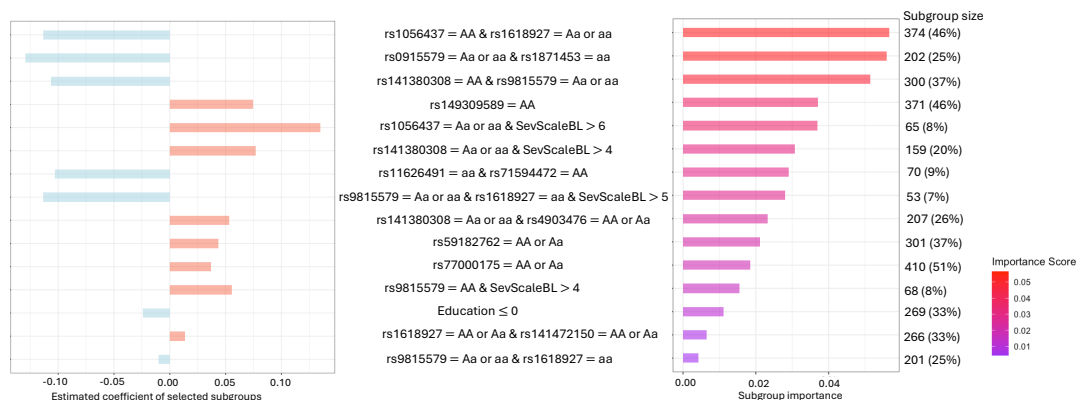


Figure 6: Subgroups identified by training the model on AREDS at year five. The right panel shows the subgroup importance ordered by the subgroup importance score. Subgroup size in AREDS is listed on the right column. The left panel shows the corresponding estimated coefficients. Light blue represents negative values of the estimated coefficients; orange represents positive values of the estimated coefficients.  $\alpha$  was set as 0.01 without Bonferroni corrections for generating candidate subgroups in gradient boosting CTree.

The top three subgroups with the highest subgroup importance scores show adverse effects (e.g., negative estimated coefficients). In AREDS trial, the top 1 beneficial subgroup (complementary to “ $rs1056437 = AA$  and  $rs1618927 = Aa$  or  $aa$ ”) has 432 (54%) patients, the top 2 beneficial subgroup (complementary to “ $rs9815579 = Aa$  or  $aa$  and  $rs1871453 = aa$ ”) has 604 (75%) patients, and the top 3 beneficial subgroup (complementary to “ $rs141380308 = AA$  and  $rs9815579 = Aa$  or  $aa$ ”) has 506 (63%) patients. 355 (44%) patients were in both top 1 and top 2 beneficial subgroups and 247 (31%) patients were in all top three beneficial subgroups.

We then validated the results on AREDS2 trial. The top 1 beneficial subgroup has 62 (56%) patients, the top 2 beneficial subgroup has 79 (72%) patients, and the top 3 beneficial subgroup has 74 (67%) patients. 52 (47%) patients were in the top 1 and top 2 beneficial subgroups and 38 (35%) patients were in all top three beneficial subgroups. We plotted KM curves by beneficial subgroup vs “adverse” subgroup for the top three subgroups on AREDS2 (the upper panel of Figure 7). KM curves are obviously separable by identified subgroups (p-value = 0.03 by subgroup “ $rs1056437 = AA$  and  $rs1618927 = Aa$  or  $aa$ ”; 0.042 by subgroup “ $rs9815579 = Aa$  or  $aa$  and  $rs1871453 = aa$ ”). Although the log-rank test by subgroup “ $rs141380308 = AA$  and  $rs9815579 = Aa$  or  $aa$ ” is not statistically significant, the KM curves still show a clear separation. The lower panel of Figure 7 shows the distribution of predicted CATEs on AREDS2 by each of the top three subgroups. The predicted CATEs show obvious differences for patients in the beneficial subgroup vs “adverse” subgroup ( $p < 0.05$  for all three). Most individuals in the beneficial subgroups have positive predicted CATE values, while most individuals in the “adverse” subgroups have negative predicted CATE values. This

effectively illustrates treatment heterogeneity, validating the capability of simultaneous estimation of CATE and identification of subgroups through our proposed algorithm.

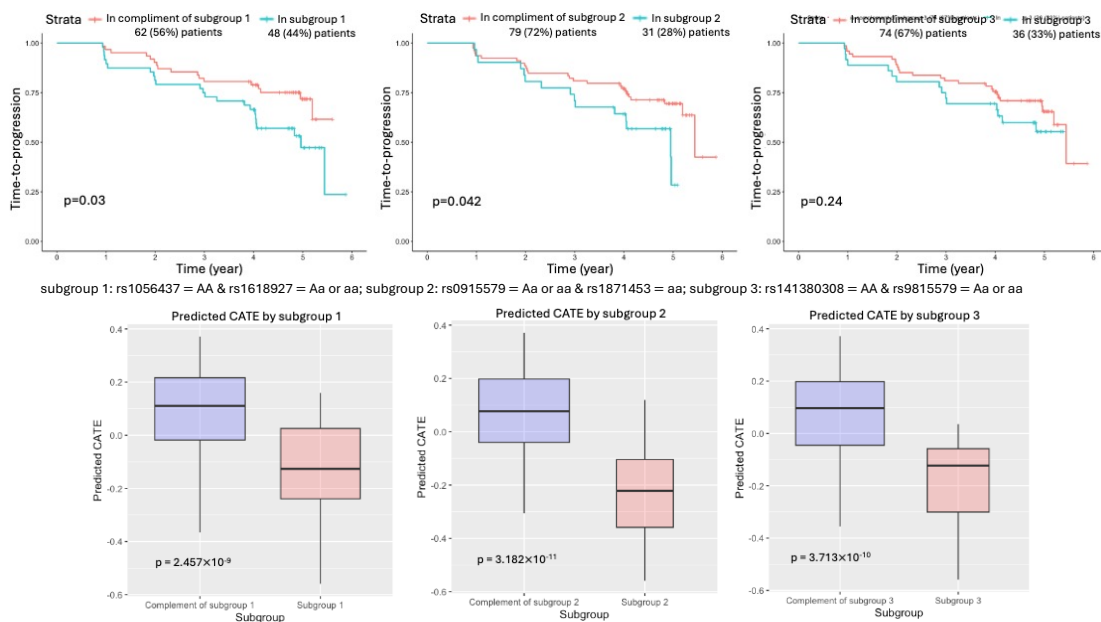


Figure 7: Validation results on AREDS2. The upper panel shows KM curves on AREDS2 by the top three subgroups identified by training the algorithm on AREDS with  $\alpha = 0.01$  but no Bonferroni corrections in gradient boosting CTree for generating candidate subgroups. P-values shown on the plots were calculated from log-rank tests to compare the survival curves for patients between beneficial vs “adverse” subgroups. The lower panel shows the distributions of predicted CATEs on AREDS2 plotted by the top three subgroups. The width of the boxes represent the sample size in the beneficial and “adverse” subgroups. P-values were calculated by performing Wilcoxon rank sum tests.

## 6 Conclusions and Discussions

In this paper, we proposed an interpretable HTE estimation framework for estimating CATE in survival outcomes with causal subgroup discovery. We examined the performance of three meta-learners for constructing pseudo-ITE coupled with the conditional inference tree to simultaneously estimate CATE and identify subgroups under independent and weakly correlated signal settings. We recommend DEA-learner to construct pseudo-ITE which shows the best performance in terms of subgroup identification accuracy while maintaining a good prediction accuracy. We then applied the proposed framework under DEA-learner to the AREDS trial and identified SNP-based subgroups and treatment heterogeneity. Our findings were verified through analysis of AREDS2, an independent test dataset.

One limitation of our proposed method is that the choice of time of interest might affect the magnitude of subgroup effects. Prior knowledge or preliminary analysis is needed to determine a meaningful time of

interests. In addition, it is unavoidable to choose whether to use multiple testing adjustments or not and to choose a  $\alpha$  level for the splitting rule in CTree. Although we made recommendations through simulation studies under various scenarios, the choice of  $\alpha$  is still subjective. A strict  $\alpha$  level yields sparse subgroups, but may lose important information, while a relaxed  $\alpha$  level might yield many subgroups with small effect sizes. Through our experiences in the real data analysis, the top subgroups (with high subgroup important scores) always almost retain the same whichever the  $\alpha$  level is. We also recommend additional survival analysis to examine the effects of identified subgroups for a post-hoc screening. Furthermore, our proposed method assumes no unmeasured confounders, which means that our method may not perform well in observational data settings (e.g., electronic health records) unless a sufficiently large number of covariates are collected. We will further investigate this direction by adapting the proposed method to observational studies.

## References

- Falco J. Bargagli-Stoffi, Riccardo Cadei, Kwonsang Lee, and Francesca Dominici. Causal rule ensemble: Interpretable discovery and inference of heterogeneous treatment effects, 2024. URL <https://arxiv.org/abs/2009.09036>.
- Na Bo, Jong-Hyeon Jeong, Erick Forno, and Ying Ding. A pseudo-outcome-based framework to analyze treatment heterogeneity in survival data using electronic health records, 2024a. URL <https://arxiv.org/abs/2407.01565>.
- Na Bo, Yue Wei, Lang Zeng, Chaeryon Kang, and Ying Ding. A meta-learner framework to estimate individualized treatment effects for survival outcomes. *Journal of Data Science*, pages 1–19, 2024b. ISSN 1680-743X. doi: 10.6339/24-JDS1119.
- Shuai Chen, Lu Tian, Tianxi Cai, and Menggang Yu. A general statistical framework for subgroup identification and comparative treatment scoring. *Biometrics*, 73(4):1199–1209, 2017. doi: <https://doi.org/10.1111/biom.12676>. URL <https://onlinelibrary.wiley.com/doi/abs/10.1111/biom.12676>.
- Victor Chernozhukov, Denis Chetverikov, Mert Demirer, Esther Duflo, Christian Hansen, Whitney Newey, and James Robins. Double/debiased machine learning for treatment and structural parameters. *The Econometrics Journal*, 21(1):C1–C68, 01 2018. ISSN 1368-4221. doi: 10.1111/ectj.12097. URL <https://doi.org/10.1111/ectj.12097>.
- Yifan Cui, Michael R Kosorok, Erik Sverdrup, Stefan Wager, and Ruoqing Zhu. Estimating heterogeneous treatment effects with right-censored data via causal survival forests. *Journal of the Royal Statistical*

- Society Series B: Statistical Methodology*, 02 2023. ISSN 1369-7412. doi: 10.1093/jrsssb/qkac001. URL <https://doi.org/10.1093/jrsssb/qkac001>. qkac001.
- Jerome H. Friedman and Bogdan E. Popescu. Predictive learning via rule ensembles. *The Annals of Applied Statistics*, 2(3):916–954, 2008. ISSN 19326157. URL <http://www.jstor.org/stable/30245114>.
- Mayu Hiraishi, Ke Wan, Kensuke Tanioka, Hiroshi Yadohisa, and Toshio Shimokawa. Causal rule ensemble method for estimating heterogeneous treatment effect with consideration of prognostic effects. *Statistical Methods in Medical Research*, 33(6):1021–1042, 2024. doi: 10.1177/09622802241247728. URL <https://doi.org/10.1177/09622802241247728>. PMID: 38676367.
- Torsten Hothorn, Kurt Hornik, and Achim Zeileis. Unbiased recursive partitioning: A conditional inference framework. *Journal of Computational and Graphical Statistics*, 15(3):651–674, 2006. doi: 10.1198/106186006X133933. URL <https://doi.org/10.1198/106186006X133933>.
- Liangyuan Hu, Jiayi Ji, and Fan Li. Estimating heterogeneous survival treatment effect in observational data using machine learning. *Statistics in Medicine*, 40(21):4691–4713, 2021. doi: <https://doi.org/10.1002/sim.9090>. URL <https://onlinelibrary.wiley.com/doi/abs/10.1002/sim.9090>.
- Liangyuan Hu, Jiayi Ji, Ronald D. Ennis, and Joseph W. Hogan. A flexible approach for causal inference with multiple treatments and clustered survival outcomes. *Statistics in Medicine*, 41(25):4982–4999, 2022a. doi: <https://doi.org/10.1002/sim.9548>. URL <https://onlinelibrary.wiley.com/doi/abs/10.1002/sim.9548>.
- Liangyuan Hu, Jiayi Ji, Ronald D. Ennis, and Joseph W. Hogan. A flexible approach for causal inference with multiple treatments and clustered survival outcomes. *Statistics in Medicine*, 41(25):4982–4999, 2022b. doi: <https://doi.org/10.1002/sim.9548>. URL <https://onlinelibrary.wiley.com/doi/abs/10.1002/sim.9548>.
- Edward H. Kennedy. Towards optimal doubly robust estimation of heterogeneous causal effects. *arXiv:2004.14497*, 2020.
- X Nie and S Wager. Quasi-oracle estimation of heterogeneous treatment effects. *Biometrika*, 108(2):299–319, 09 2020. ISSN 0006-3444. doi: 10.1093/biomet/asaa076. URL <https://doi.org/10.1093/biomet/asaa076>.
- Donald B Rubin. Estimating causal effects of treatments in randomized and nonrandomized studies. *Journal of Educational Psychology*, 66(4):688–701, 1974.

- J. Splawa-Neyman, D.M. Dabrowska, and T. Speed. On the application of probability theory to agricultural experiments. essay on principles. *Statistical Science*, 5(4):465–472, 1990.
- Lu Tian, Ash A. Alizadeh, Andrew J. Gentles, and Robert Tibshirani. A simple method for estimating interactions between a treatment and a large number of covariates. *Journal of the American Statistical Association*, 109(508):1517–1532, 2014. doi: 10.1080/01621459.2014.951443. URL <https://doi.org/10.1080/01621459.2014.951443>. PMID: 25729117.
- Ke Wan, Kensuke Tanioka, and Toshio Shimokawa. Rule ensemble method with adaptive group lasso for heterogeneous treatment effect estimation. *Statistics in Medicine*, 42(19):3413–3442, 2023a. doi: <https://doi.org/10.1002/sim.9812>. URL <https://onlinelibrary.wiley.com/doi/abs/10.1002/sim.9812>.
- Ke Wan, Kensuke Tanioka, and Toshio Shimokawa. Survival causal rule ensemble method considering the main effect for estimating heterogeneous treatment effects, 2023b. URL <https://arxiv.org/abs/2309.11914>.
- Yue Wei, Jason C. Hsu, Wei Chen, Emily Y. Chew, and Ying Ding. Identification and inference for subgroups with differential treatment efficacy from randomized controlled trials with survival outcomes through multiple testing. *Statistics in Medicine*, 40(29):6523–6540, 2021.
- Ying Wu, Hanzhong Liu, Kai Ren, and Xiangyu Chang. Causal rule learning: Enhancing the understanding of heterogeneous treatment effect via weighted causal rules, 2023. URL <https://arxiv.org/abs/2310.06746>.
- Qi Yan, Ying Ding, Yi Liu, Tao Sun, Lars G Fritsche, Traci Clemons, Rinki Ratnapriya, Michael L Klein, Richard J Cook, Yu Liu, Ruzong Fan, Lai Wei, Gonçalo R Abecasis, Anand Swaroop, Emily Y Chew, AREDS2 Research Group, Daniel E Weeks, and Wei Chen. Genome-wide analysis of disease progression in age-related macular degeneration. *Human Molecular Genetics*, 27(5):929–940, 2018.